JOURNAL OF THE AMERICAN COLLEGE OF CARDIOLOGY
© 2015 BY THE AMERICAN COLLEGE OF CARDIOLOGY FOUNDATION
PUBLISHED BY ELSEVIER INC.

VOL. 65, NO. 23, 2015
ISSN 0735-1097/$36.00
http://dx.doi.org/10.1016/j.jacc.2015.04.020

ORIGINAL INVESTIGATIONS

Vasa Vasorum Restructuring in Human Atherosclerotic Plaque Vulnerability

A Clinical Optical Coherence Tomography Study

Akira Taruya, MD, Atsushi Tanaka, MD, PhD, Tsuyoshi Nishiguchi, MD, Yoshiki Matsuo, MD, PhD, Yuichi Ozaki, MD, PhD, Manabu Kashiwagi, MD, PhD, Yasutsugu Shiono, MD, Makoto Orii, MD, Takashi Yamano, MD, Yasushi Ino, MD, Kumiko Hirata, MD, PhD, Takashi Kubo, MD, PhD, Takashi Akasaka, MD, PhD

ABSTRACT

BACKGROUND Previous studies have suggested that vasa vasorum (VV) is associated with plaque progression and vulnerability.

OBJECTIVES The aim of this study was to investigate the relationship between coronary neovascularization structures and plaque characteristics.

METHODS We included 53 patients who underwent optical coherence tomography to observe the proximal left anterior descending coronary artery. Patients were classified into 5 groups according to lesion characteristics: normal; fibrous plaque (FP); fibroatheroma (FA); plaque rupture (PR); and fibrocalcific plaque (FC). We defined signal-poor tubuloluminal structures recognized in cross-sectional and longitudinal profiles located in adventitial layer as VV, and within plaque as intraplaque neovessels. Two types of longitudinal microvascular structure (external running and internal running) and a particular type of intraplaque neovessels (a coral tree pattern) were noted. All VV and intraplaque neovessels were manually segmented followed by quantification with Simpson method.

RESULTS Among the groups, there was significant difference (expressed as median [interquartile range (IQR)]) in VV volume (normal: 0.329 [IQR: 0.209 to 0.361] mm^3, FP: 0.433 [IQR: 0.297 to 0.706] mm^3, FA: 0.288 [IQR: 0.113 to 0.364] mm^3, PR: 0.160 [IQR: 0.141 to 0.193] mm^3, and FC: 0.106 [IQR: 0.053 to 0.165] mm^3; $p = 0.003$) and intraplaque neovessels volume (normal: 0.00 [IQR: 0.00 to 0.00] mm^3, FP: 0.00 [IQR: 0.00 to 0.00] mm^3, FA: 0.028 [IQR: 0.019 to 0.041] mm^3, PR: 0.035 [IQR: 0.026 to 0.042] mm^3, and FC: 0.010 [IQR: 0.005 to 0.014] mm^3; $p < 0.001$). Significant differences were observed in the prevalence of the internal running (normal: 0.0%, FP: 28.6%, FA: 40.0%, PR: 70.0%, and FC: 40.0%; $p = 0.032$) and the coral tree pattern (normal: 0.0%, FP: 7.1%, FA: 40.0%, PR: 80.0%, and FC: 10.0%; $p < 0.01$). The VV volume correlated with fibrous plaque volume ($r = 0.71$; $p < 0.01$).

CONCLUSIONS VV increase with fibrous plaque volume and intraplaque neovessels with particular structures are associated with plaque vulnerability. Imaging for microvasculature could become a new window for plaque vulnerability. (J Am Coll Cardiol 2015;65:2469–77) © 2015 by the American College of Cardiology Foundation.

From the Department of Cardiovascular Medicine, Wakayama Medical University, Wakayama, Japan. This work was supported by JSPS KAKENHI Grant Number 24591068. Dr. Akasaka is an advisory board member of St. Jude Medical and Terumo; and receives research support from Abbott Vascular Japan, St. Jude Medical Japan, and Terumo. All other authors have reported that they have no relationships relevant to the contents of this paper to disclose.
Listen to this manuscript's audio summary by *JACC* Editor-in-Chief Dr. Valentin Fuster.

Manuscript received December 30, 2014; revised manuscript received March 13, 2015, accepted April 7, 2015.

ABBREVIATIONS AND ACRONYMS

3D = 3-dimensional
FA = fibroatheroma
FC = fibrocalcific plaque
FD = frequency domain
FP = fibrous plaque
IQR = interquartile range
LAD = left anterior descending coronary artery
OCT = optical coherence tomography
PR = plaque rupture
VV = vasa vasorum

Previous studies have suggested that the vasa vasorum (VV) neovascularization could play a key role in the development of human atherosclerotic plaque (1–4). In addition to plaque progression, it has reported that intraplaque neovascularization is closely associated with plaque vulnerability (5). Due to the lack of adequate in vivo imaging tool for microvasculatures in coronary artery, however, little is known about relationship between structures of in vivo human coronary microvasculature and plaque characteristics.

SEE PAGE 2478

Optical coherence tomography (OCT) is a light-based imaging modality that generates high-resolution cross-sectional images of tissue microstructure (6). Because the spatial resolution of current commercially available OCT, namely frequency-domain OCT (FD-OCT), is sharp enough to detect microvasculatures, recent studies have suggested that coronary VV and intraplaque neovessels could be detected as a microchannel in an FD-OCT image (7,8).

The aim of this study was to investigate the relationship between the structure of microvasculatures and plaque characteristics using FD-OCT in patients with coronary artery disease.

FIGURE 1 Adventitial VV by OCT in Normal Coronary Artery

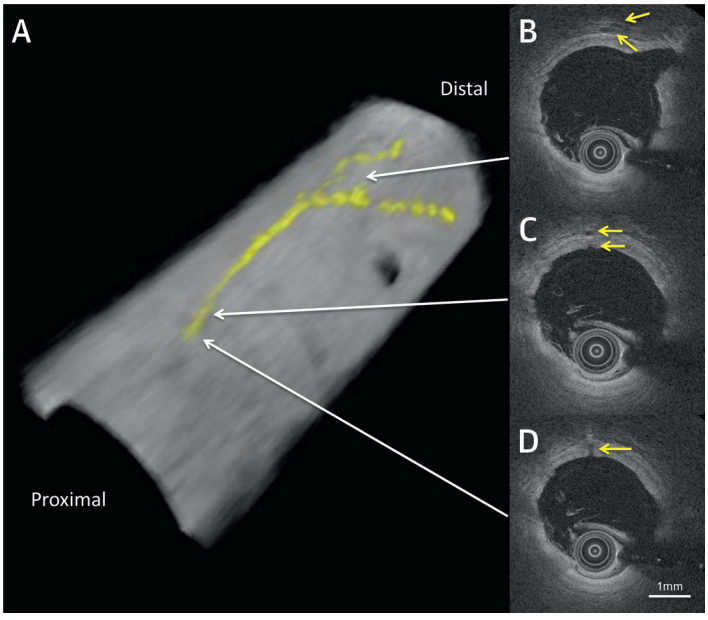

(A) Three-dimensional rendering of optical coherence tomography (OCT) images for a longitudinal running of adventitial vasa vasorum (VV), highlighted in **yellow**. **(B to D)** Cross-sectional images of OCT for VV **(yellow arrow)**. Adventitial VV runs longitudinally **(A)** along the adventitial layer **(B,C)**. The cross-sectional images show that the left anterior descending artery directly branches off the VV **(C,D)**.

METHODS

STUDY POPULATION. We included 346 patients who underwent FD-OCT to observe the proximal left anterior descending coronary artery (LAD) before percutaneous coronary intervention between February 1, 2012, and October 31, 2014 at Wakayama Medical University Hospital. Then, we excluded participants who had the following: 1) a history of previous percutaneous coronary intervention or bypass surgery on LAD (n = 63); 2) LAD with distal lesion (n = 23); 3) lesion with thrombus (n = 102); 4) target vessel reference diameter of >4 mm (n = 51); or 5) poor OCT images for VV analysis (n = 54). Ultimately, we analyzed 53 patients for this study.

This study complies with the Declaration of Helsinki and was approved by the Ethics Committee of Wakayama Medial University. We also obtained written informed consent from all participants before initial coronary angiography.

OCT IMAGE ACQUISITION. After coronary angiography and before percutaneous coronary intervention, FD-OCT imaging was performed using a 6-F guiding catheter. An FD-OCT catheter (FastView, Terumo, Tokyo, Japan; or C7 Dragonfly, St. Jude Medical, St. Paul, Minnesota) was advanced to the distal LAD. In order to remove blood cells from the view area, contrast medium was continuously flushed from the guiding catheter when the OCT was imaged using automatic pullback devices at 20 mm/s. Following previous studies (7,9), we used the FD-OCT image of the proximal LAD in a 10-mm length.

All OCT data were digitally stored and transferred to ImageJ (U.S. National Institutes of Health, Bethesda, Maryland) for 2-dimensional image analysis and to OsiriX (Pixmeo SARL, Bernex, Switzerland) for 3-dimensional (3D) rendering.

OCT IMAGE ANALYSIS. We classified lesion characteristics into 5 groups according to the consensus documents of OCT (10): normal; fibrous plaque (FP); fibroatheroma (FA); plaque rupture (PR); and fibrocalcific plaque (FC). Briefly, the normal vessel wall is characterized by a layered architecture, comprising a highly backscattered or signal-rich intima, a medium that frequently has low backscattering or is signal-poor, and a heterogeneous and frequently highly backscattering adventitia. FP has high backscattering and a relatively homogeneous OCT signal. FA is defined as a mass lesion or loss of a layered structure of the vessel wall resulting from a necrotic core. The plaque rupture was defined as the presence of fibrous

cap discontinuity and a cavity formation in the plaque (11). FC contains fibrous tissue, along with calcium that appears as a signal-poor or heterogeneous region with a sharply delineated border. Depending on the plaque characteristics of the proximal LAD, patients were divided into 5 groups: a normal group (n = 9); an FP group (n = 14); an FA group (n = 10); a PR group (n = 10); and an FC group (n = 10).

IMAGE ANALYSIS FOR NEOVASCULARIZATION. We defined signal-poor tubuloluminal structures recognized in cross-sectional and longitudinal profiles, which were located in the adventitial layer as VV, and within plaque as intraplaque neovessels (10,12). When more than 1 mm of longitudinal running structure of VV or intraplaque neovessels was observed, we classified it into 1 of 2 types depending on the location: an external running type located in the adventitia (Figure 1) and an internal running type mainly located within plaque (Figure 2). In 3D OCT images, we noted the particular type of intraplaque neovessels that was from the adventitia or coronary artery branches following a distinct pattern of arborization and entering plaque as a coral tree pattern (Figure 3). Semiquantified macrophage grading system was applied (13).

All cross-sectional images served for this study were generated from A-line data (raw data) using ImageJ. All VV and intraplaque neovessels were manually segmented. Then, the VV and intraplaque vessels areas were individually measured by the automated analysis system of ImageJ. The VV volume and intraplaque neovessels volume were calculated by integrating all of the cross-sectional area measurements multiplied by the slice thickness (Simpson rule).

REPRODUCIBILITY FOR VASA VASORUM VOLUME ASSESSMENT. Interobserver variability for the assessment of VV volume was analyzed in 20 randomly selected cases by 2 independent observers (A. Taruya and T. Nishiguchi). Repeated measurement for 20 cases by 1 observer (A. Taruya) was performed for intraobserver variability analysis 2 months after the first measurement.

STATISTICAL ANALYSIS. Continuous variables are expressed as mean ± SD or median (interquartile range [IQR]), and categorical variables are expressed as number (%). We used chi-square test for categorical variables and one-way analysis of variance tests for continuous variables to assess differences in the plaque characteristics. Medians of VV volume and intraplaque neovessels volume were compared using Kruskal-Wallis test. If there was a significant difference with Kruskal-Wallis test, a post-hoc test using Dunn multiple-comparison test was employed. Categorical variables were compared with chi-square test. A single-regression analysis was applied to assess the relationship between the VV volume and the plaque volume. Bland-Altman test was used for the reproducibility of VV volume assessment. A p value of <0.05 was considered significant.

FIGURE 2 Intraplaque Neovessels by OCT in a Ruptured Plaque

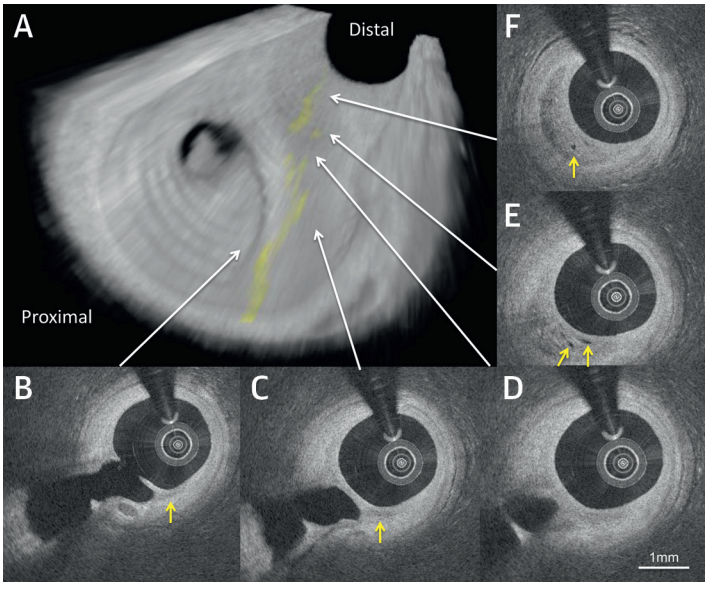

(A) Cutaway view of a 3-dimensional transmissive-rendering optical coherence tomography (OCT) image for a longitudinal running of intraplaque neovessels, highlighted in **yellow**. **(B to F)** Cross-sectional images of OCT for intraplaque neovessels **(yellow arrow)** in a ruptured plaque. A straight running of intraplaque neovessels **(A)** are abruptly interrupted just at the rupture site **(D)**. In cross-sectional images, intraplaque neovessels run along the plaque shoulder **(B,C)** in the proximal site of the plaque rupture and seem to reappear from the rupture cavity in the distal rupture site **(E,F)**. Intraplaque neovessels look to be a break point for plaque rupture.

RESULTS

PATIENT CHARACTERISTICS. The patients' characteristics are summarized in Table 1. There was no significant difference in the patients' characteristics between the groups.

VASA VASORUM AND PLAQUE CHARACTERISTICS. Figure 4A shows the VV volume in each plaque characteristic. There was significant difference in the VV volume among the 5 groups (normal: 0.329 [IQR: 0.209 to 0.361] mm^3, FP: 0.433 [IQR: 0.297 to 0.706] mm^3, FA: 0.288 [IQR: 0.113 to 0.364] mm^3, PR: 0.160 [IQR: 0.141 to 0.193] mm^3, and FC: 0.106 [IQR: 0.053 to 0.165] mm^3; p = 0.003). According to the post-hoc test, the VV volume of the FP was larger than that of the FC ($p < 0.05$).

No statistical difference was observed in an average number of VV per slice (normal: 12.9 [IQR: 7.9 to 16.4], FP: 16.8 [IQR: 8.1 to 24.3], FA: 9.1 [IQR: 6.6 to 15.7], PR: 7.8 [IQR: 3.6 to 10.7], and FC: 10.3 [IQR: 6.2 to 12.7]; p = 0.20).

FIGURE 3 A Coral Tree Pattern of Intraplaque VV Toward an FA

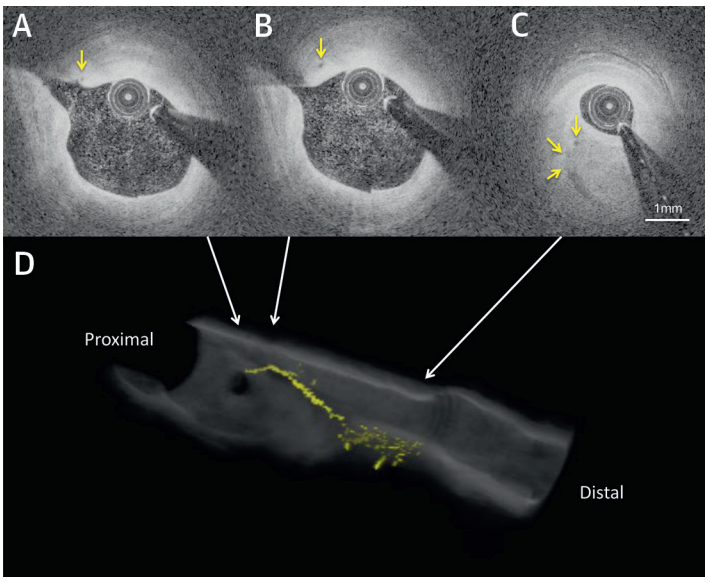

(A to C) Cross-sectional images of optical coherence tomography (OCT) for intraplaque neovessels **(yellow arrow). (D)** Cutaway view of 3-dimensional transmissive-rendering OCT image for a coral tree pattern, highlighted in **yellow**. Intraplaque neovessels originating from the coronary artery branch **(A,B)** run spirally in a longitudinal direction **(D)** and enter the fibroatheroma (FA) **(C)** with ramification like a coral tree **(D)**.

INTRAPLAQUE NEOVESSELS AND PLAQUE CHARACTERISTICS. Figure 4B shows the intraplaque neovessels volume in each plaque characteristic. There was significant difference in the intraplaque neovessels volume among the 5 groups (normal: 0.00 [IQR: 0.00 to 0.00] mm^3, FP: 0.00 [IQR: 0.00 to 0.00] mm^3, FA: 0.028 [IQR: 0.019 to 0.041] mm^3, PR: 0.035 [IQR: 0.026 to 0.042] mm^3, and FC: 0.010 [IQR: 0.005 to 0.014] mm^3; $p < 0.001$). Post-hoc analysis revealed that the intraplaque neovessels volume in the FA and PR groups were larger than that in the FP ($p < 0.05$).

There was statistical difference in an average number of intraplaque neovessels per slice (normal: 0.0 [IQR: 0.0 to 0.0], FP: 0.0 [IQR: 0.0 to 0.0], FA: 0.54 [IQR: 0.10 to 1.08], PR: 0.37 [IQR: 0.25 to 0.80], and FC: 0.27 [IQR: 0.07 to 0.49]; $p < 0.01$). By post-hoc analysis, the average numbers of intraplaque neovessels per slice in the FA and PR were larger compared with that in the FP ($p < 0.05$).

THE LONGITUDINAL RUNNING STRUCTURE AND CORAL TREE PATTERN. The prevalence of the longitudinal running structures and the coral tree pattern are summarized in Figure 5. Whereas the prevalence of the external running type was similar among the groups (normal: 77.8%, FP: 78.6%, FA: 80.0%, PR: 60.0%, and FC: 70.0%; $p = 0.83$), that of the internal running type was statistically different among the groups (normal: 0.0%, FP: 28.6%, FA: 40.0%, PR: 70.0%, and FC: 40.0%; $p = 0.032$). There was significant difference in the prevalence of the coral tree pattern among the groups (normal: 0.0%, FP: 7.1%, FA: 40.0%, PR: 80.0%, and FC: 10.0%; $p < 0.01$). The lesion with the coral tree pattern showed higher average macrophage grade per slice (with a coral tree pattern 1.90 [1.20 to 2.20] vs. without a coral tree pattern 0.40 [0.05 to 1.20]; $p < 0.0001$).

TABLE 1 Baseline Clinical Characteristics

	Normal Group (n = 9)	FP Group (n = 14)	FA Group (n = 10)	PR Group (n = 10)	FC Group (n = 10)	p Value
Age, yrs	58.3 ± 5.9	59.9 ± 17.2	73.6 ± 6.3	68.2 ± 9.9	71.9 ± 8.6	0.37
Male	8 (88.9)	12 (85.7)	9 (90.0)	7 (70.0)	5 (50.0)	0.25
DM	1 (11.1)	6 (42.9)	3 (30.0)	5 (50.0)	4 (40.0)	0.40
HT	5 (55.6)	9 (64.3)	7 (70.0)	9 (90.0)	7 (70.0)	0.35
DLP	5 (55.6)	7 (50.0)	4 (40.0)	6 (60.0)	5 (50.0)	0.94
Smoking	6 (66.7)	7 (50.0)	5 (50.0)	6 (60.0)	3 (30.0)	0.79
Family history of CAD	3 (33.3)	3 (21.4)	3 (30.0)	2 (20.0)	2 (20.0)	0.93
BMI, kg/m^2	22.9 ± 3.0	25.1 ± 4.9	22.2 ± 2.7	23.3 ± 3.0	24.4 ± 3.3	0.57
Cr, mg/dl	0.8 (0.6–0.9)	0.9 (0.7–1.0)	0.9 (0.6–1.4)	0.9 (0.8–1.4)	0.7 (0.7–1.0)	0.36
BUN, mg/dl	15.0 (13.0–17.5)	15.5 (12.0–19.0)	18.8 (14.0–27.0)	15.5 (11.0–19.5)	17.7 (17.0–22.0)	0.17
LDL-C, mg/dl	93 (77–117)	107 (70–120)	93 (66–143)	122 (75–129)	93 (86–108)	0.87
HDL-C, mg/dl	42 (40–47)	38 (35–53)	44 (39–54)	37 (30–52)	41 (36–43)	0.51
TG, mg/dl	96 (92–162)	110 (74–217)	105 (92–115)	117 (102–132)	112 (92–151)	0.78
HbA1c, %	5.6 ± 0.5	6.2 ± 0.7	6.3 ± 0.9	6.5 ± 0.9	6.6 ± 1.0	0.10
logCPR, mg/dl	−1.1 ± 0.5	−0.6 ± 0.5	−0.5 ± 0.6	−1.0 ± 0.5	−1.4 ± 0.2	0.11

Values are mean ± SD, n (%), or median (interquartile range).

BMI = body mass index; BUN = blood urea nitrogen; CAD = coronary artery disease; Cr = creatinine; CRP = C-reactive protein; DLP = dyslipidemia; DM = diabetes mellitus; FA = fibroatheroma; FC = fibrocalcific plaque; FP = fibrous plaque; HbA1c = glycated hemoglobin A1c; HDL-C = high-density lipoprotein cholesterol; HT = hypertension; LDL-C = low-density lipoprotein cholesterol; PR = plaque rupture; TG = triglyceride.

FIGURE 4 Adventitial VV and Intraplaque Neovessels Volume by OCT Among Plaque Characteristics

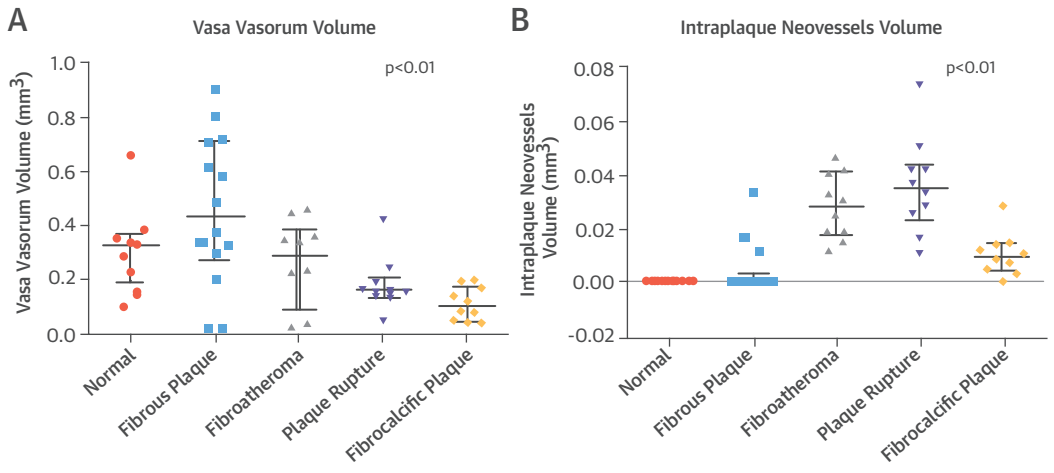

Adventitial VV **(A)** and intraplaque neovessels volume **(B)** of each plaque characteristic are shown. The **bar** shows the median and interquartile range. There is a significant difference in the volume of adventitial VV and intraplaque neovessels among the plaque characteristics. Abbreviations as in Figure 1.

VASA VASORUM AND PLAQUE VOLUME. Figure 6A shows the relationship between the VV volume and the plaque volume in the FP group. The VV volume was positively correlated with the plaque volume ($r = 0.71$; $p < 0.01$). In the FA and PR groups, the intraplaque neovessels volume showed modest correlation with plaque volume (Figure 6B) ($r = 0.53$; $p = 0.04$).

REPRODUCIBILITY OF THE VASA VASORUM VOLUME ASSESSMENT. The interobserver and intraobserver variability with regard to the VV volume were $r = 0.861$ and $r = 0.864$, respectively. According to Bland-Altman analysis, the 95% limits of agreement of the interobserver and intraobserver variability of VV volume were 0.02 ± 0.10 mm^3 and 0.01 ± 0.08 mm^3 (mean $\pm$ 1.96 SD, respectively) (Figure 7).

DISCUSSION

The VV and intraplaque neovessels volumes are different across plaque characteristics. The specific 3D structures of intraplaque neovessels, the internal longitudinal running and the coral tree pattern, are more frequently found in the plaque rupture. The VV volume is positively correlated with fibrous plaque volume.

VASA VASORUM AND PLAQUE VOLUME. Plaque growth is a complex and poorly understood process. In this study, we confirmed positive correlation between VV volume and plaque volume in living human coronary artery. This is very consistent with the results from previous ex vivo and animal model studies

FIGURE 5 Prevalence of Inner and External Longitudinal Running of Microvasculatures by OCT and the Coral Tree Pattern

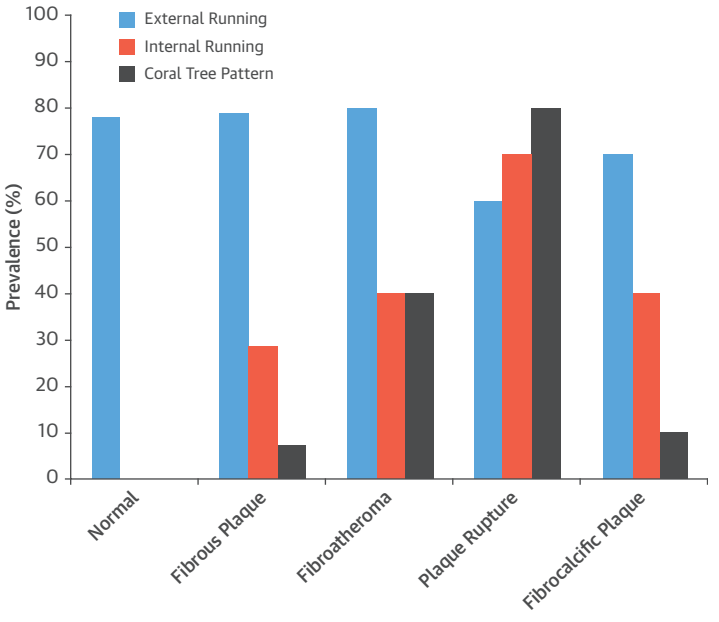

The prevalence of the external longitudinal running of VV is similar among the groups ($p = 0.83$). In contrast, that of the internal longitudinal running of intraplaque neovessels is statistically different among the groups ($p = 0.032$). There was significant difference in the prevalence of the coral tree pattern among the groups ($p < 0.01$). Abbreviations as in Figure 1.

FIGURE 6 The Relationship Between Microvasculature Volume by OCT and Plaque Volume

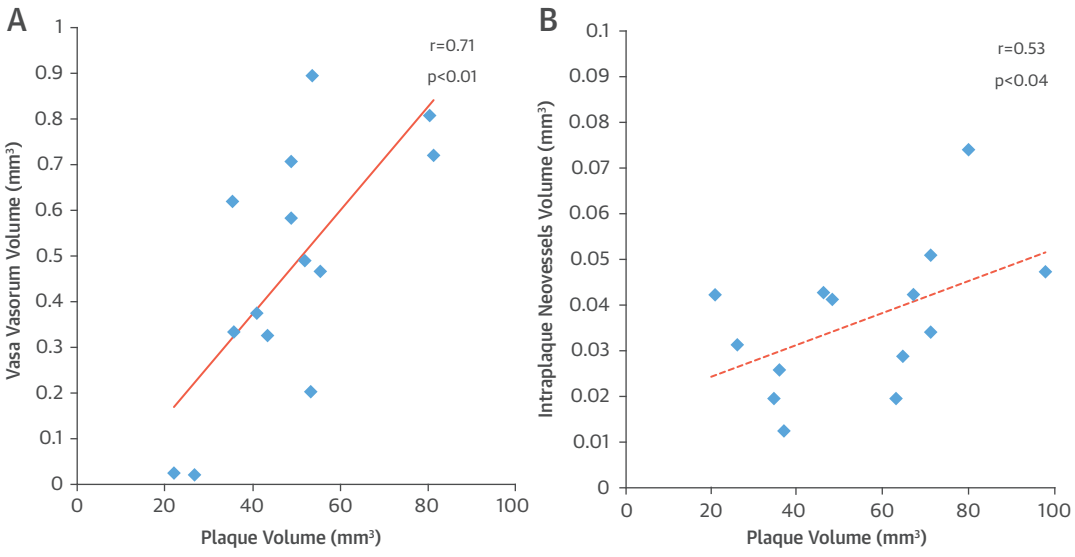

(A) VV volume is positively correlated with the plaque volume in the fibrous plaque group ($r = 0.71$; $p < 0.01$). **(B)** The relationship between intraplaque neovessels volume and the plaque volume in the FA or plaque rupture group is shown. The intraplaque neovessels volume is modestly correlated with plaque volume in the FA or plaque rupture group ($r = 0.53$; $p = 0.04$). Abbreviations as in **Figures 1 and 3**.

(14–17). In addition, we found that FP has more VV than does FC. Standing on the recent hypothesis for plaque history, FP is considered to be in the initial and progressive stage and FC in the static stage (18). As providing oxygen and nutrients from adventitia to the vessel wall is the primary role of VV (19), this positive correlation is thought to result from abundant demand of oxygen and nutrients in the progressive stage of plaque. However, several studies have suggested that the VV increasing itself promotes the plaque progression (9,15,20,21). Whether VV plays a causative or merely reactive role, VV increasing is the prologue of VV restructuring followed by further atherosclerotic change.

INTRAPLAQUE NEOVESSELS AND PLAQUE VULNERABILITY. We demonstrated that increased intraplaque neovessels were associated with plaque vulnerability. The coral tree pattern showed higher macrophage grade. These results are consistent with results from pathological studies (5,22). Several recent studies have reported that VV serve as important entry ports for the influx of cellular and noncellular proinflammatory and proatherosclerotic substances into the vessel wall (23,24) and that they in turn play a significant role in draining the arterial vessel wall (25). Considering such roles of VV, increased intraplaque neovessels volume in vulnerable plaque could be explained by the roles of VV itself and would reflect the plaque activity.

In addition, our 3D OCT more frequently found the coral tree pattern in the ruptured plaques. A pathological study reported that the size and structure of such neovasculatures were smaller and leakier compared with those of original VV (22). The leaky structure could become a break point for plaque rupture (Online Figure 1). Furthermore, a pathological study proposed that contents of necrotic core were derived from erythrocyte membrane (26). Disruption of the arborization structure of intraplaque neovessels and/or direct supply via the intraplaque neovessels, as shown in **Figure 3**, could be the main source of erythrocyte membrane for vulnerable plaque.

From a structural viewpoint, 2 types of VV have been proposed (27). One is the first-order VV arising from the lumen of the coronary artery, which ran longitudinally along the adventitial layer. The other is the smaller second-order VV that originated from branches of first-order VV or coronary artery branches and ran circumferentially to the lumen (27). In this study, the external longitudinal running similar to the first-order VV structure was found in every plaque characteristic (**Figure 1**). Very interestingly, the internal longitudinal running that mimics the first-order VV structure emerges according to changes in plaque characteristics. We speculate that the coronary artery supplements the first-order VV with neovascularization of the internal longitudinal running in response to active demand for oxygen and nutrients that a simple

FIGURE 7 Reproducibility of VV Assessment by OCT

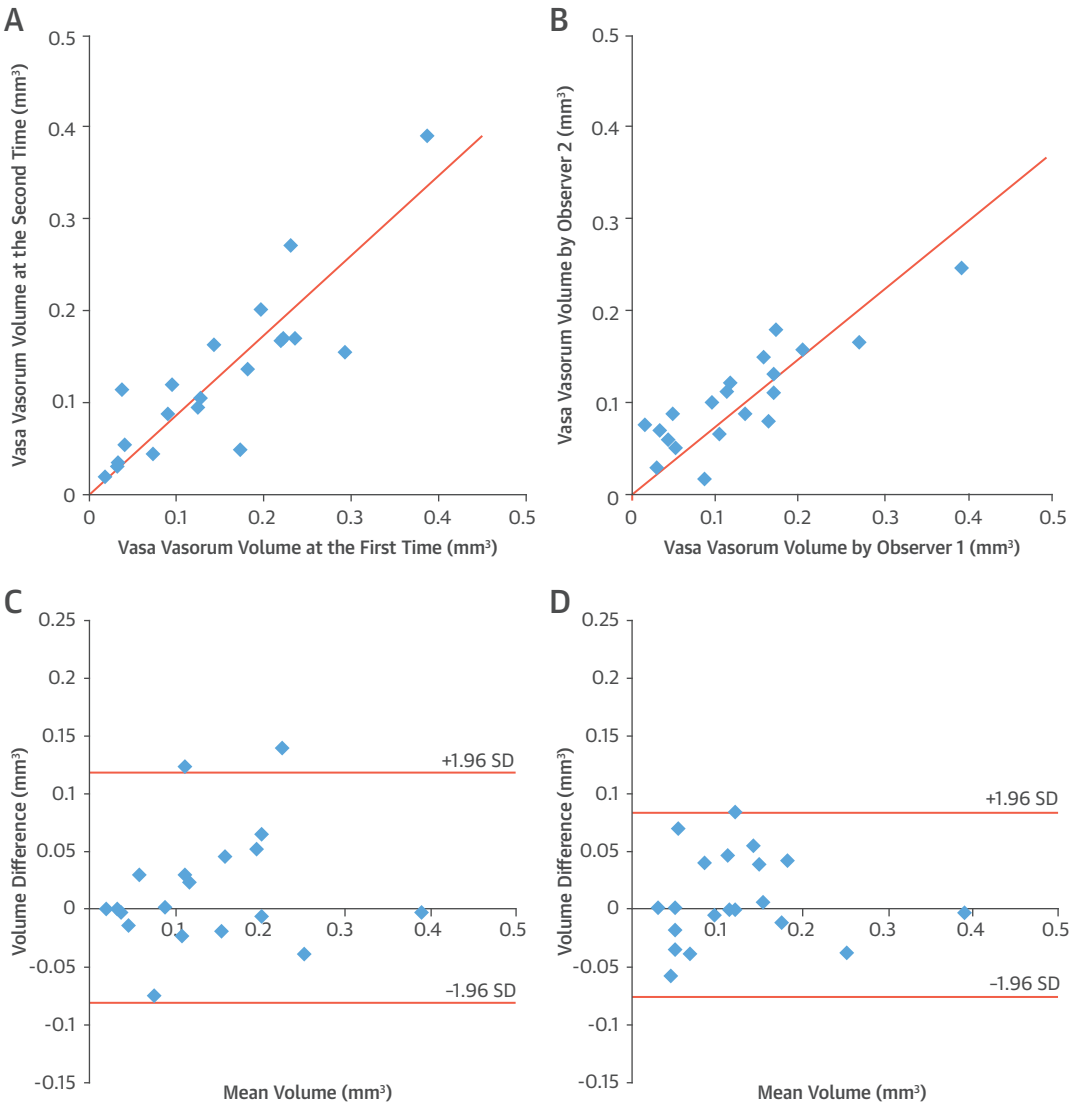

The interobserver **(A)** and intraobserver **(B)** variability of the VV volume by OCT are r = 0.861 and r = 0.864, respectively. The Bland-Altman analysis shows good agreement of the interobserver **(C)** and intraobserver **(D)** variability of VV volume assessment by OCT. Abbreviations as in Figure 1.

increase in VV cannot entirely compensate for. The 3D structural remodeling would occur in the first order level of VV (Central Illustration).

CLINICAL IMPLICATIONS. One of clinical implications of our study is the fact that the VV could become a new window for plaque vulnerability. A microcomputed tomography study showed that the mean diameter of normal first-order VV was 160.9 ± 5.10 μm; and that of second-order VV was 67.99 ± 2.72 μm (17). The results encourage us to use FD-OCT for the VV in vivo because the spatial resolution of FD-OCT is about 15 μm. The reproducibility of VV volume we achieved was sufficient for use in clinical settings.

The other clinical implication is that VV could become a new therapeutic target for coronary atherosclerotic plaque progression and instability. Drinane et al. (28) also reported that inhibition of adventitial angiogenesis by rPAI-123 decreased the number and size of second-order VV, leading to reduced plaque growth.

STUDY LIMITATIONS. First, in order to recruit high-quality OCT images for VV, only 15% of OCT cases could be analyzed. Therefore, there could be selection

CENTRAL ILLUSTRATION **VV: Plaque Characteristics and Neovascularization**

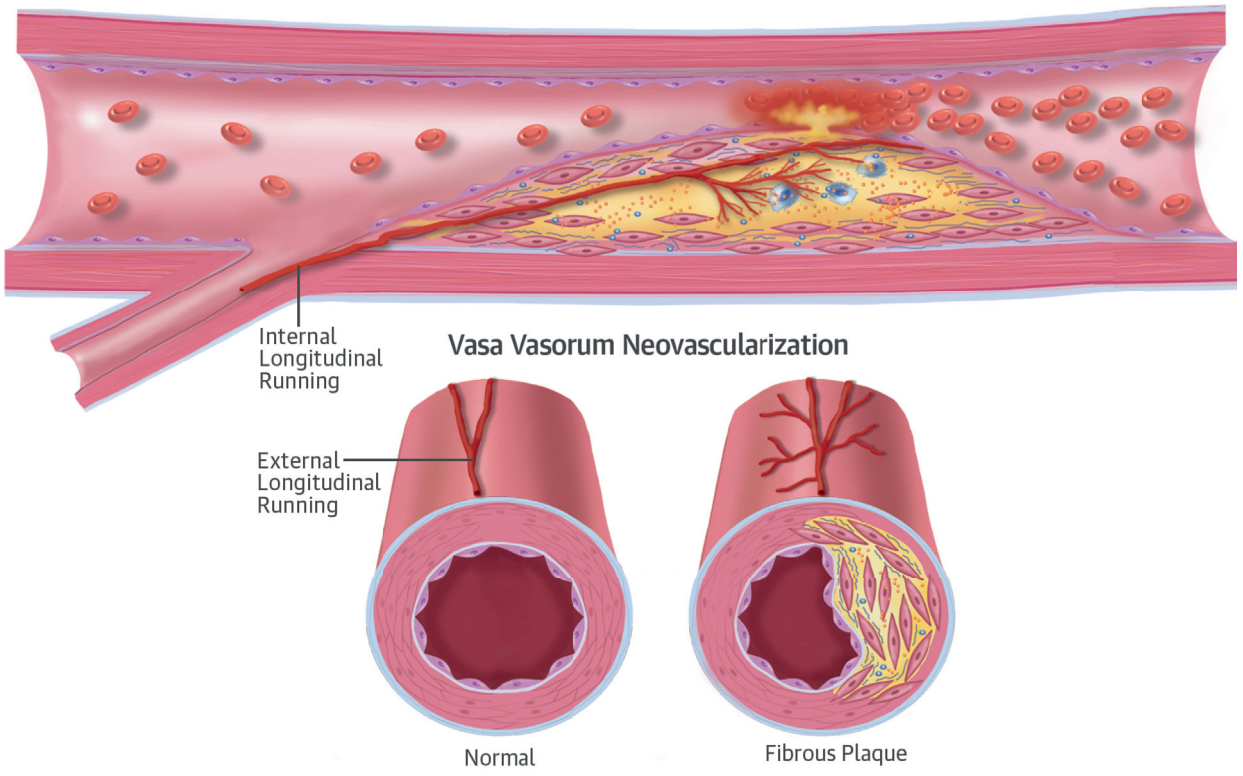

Taruya, A. et al. J Am Coll Cardiol. 2015; 65(23):2469-77.

Normal: Vasa vasorum (VV) arises from the lumen of the coronary artery, which runs longitudinally along the adventitial layer. This external longitudinal running structure can be seen in every plaque's characteristics. Fibrous plaque: VV increases with fibrous plaque growth. Fibroatheroma: An internal longitudinal running structure of intraplaque neovessels emerges according to changes in plaque characteristics. Coronary artery would supplement vasa vasorum with neovascularization of the internal longitudinal running in response to active demand for oxygen and nutrients that a simple increase in vasa vasorum cannot entirely compensate for. Plaque rupture: The coral tree pattern of intraplaque neovessels is from the adventitia or coronary artery branches following a distinct pattern of arborization and entering plaque. The leaky structure of the coral tree pattern could become a break point for plaque rupture. In addition, disruption of the arborization structure of intraplaque neovessels and/or direct supply via the intraplaque neovessels could be the main source of necrotic core for vulnerable plaque.

bias. Second, we analyzed only the proximal LAD. There is a possibility that VV structures in the right coronary artery or the circumflex would be different. Third, because FD-OCT needs lumen clearance by flushing x-ray contrast via guiding catheter, there is a possibility that FD-OCT can depict only VV closely connecting with coronary artery lumen. Furthermore, an arterial injection of the x-ray contrast results in high pressure in the arterial lumen and consequently within the arterial wall, which is consistent with Lame law. This intramural pressure gradient can result in compression of some of the VV (29). Fourth, the VV volume in the FA and PR groups might be underestimated because light signals may lose their resolution in traveling through lipid-rich plaque. Fifth, there should be debate regarding macrophage grading because not all bright spots are caused by macrophages (30,31). Finally, guidewires may have disturbed VV assessment.

CONCLUSIONS

VV increases with fibrous plaque volume. Intraplaque neovascularization with particular 3D structures, including the internal running and the coral tree pattern, are associated with plaque vulnerability. Imaging for microvasculature could become a new window for plaque vulnerability.

REPRINT REQUESTS AND CORRESPONDENCE: Dr. Atsushi Tanaka, Department of Cardiovascular Medicine, Wakayama Medical University, 811-1, Kimiidera, Wakayama 641-8509, Japan. E-mail: a-tanaka@wakayama-med.ac.jp.

PERSPECTIVES

COMPETENCY IN MEDICAL KNOWLEDGE: VV increases with FP volume, and neovascularization of intraplaque neovessels with particular structure is closely associated with plaque vulnerability.

COMPETENCY IN PATIENT CARE: VV imaging by OCT could become a new window for plaque vulnerability.

TRANSLATIONAL OUTLOOK 1: Further animal model and postmortem studies are needed to clarify the role of VV in plaque progression and vulnerability.

TRANSLATIONAL OUTLOOK 2: Serial OCT studies are necessary to establish the concept that VV imaging helps us to know plaque progression and vulnerability.

REFERENCES

1. Barger AC, Beeuwkes R 3rd, Lainey LL, Silverman KJ. Hypothesis: vasa vasorum and neovascularization of human coronary arteries: a possible role in the pathophysiology of atherosclerosis. N Engl J Med 1984;310:175–7.

2. Shi Y, O'Brien JE, Fard A, Mannion JD, Wang D, Zalewski A. Adventitial myofibroblasts contribute to neointimal formation in injured porcine coronary arteries. Circulation 1996;94:1655–64.

3. Narula J, Finn AV, Demaria AN. Picking plaques that pop…. J Am Coll Cardiol 2005;45:1970–3.

4. Moreno PR, Purushothaman KR, Sirol M, Levy AP, Fuster B. Neovascularization in human atherosclerosis. Circulation 2006;113:2245–52.

5. Moreno PR, Purushothaman KR, Fuster V, et al. Plaque neovascularization is increased in ruptured atherosclerotic lesions of human aorta: implication for plaque vulnerability. Circulation 2004;110:2032–8.

6. Hang D, Swanson EA, Lin CP, et al. Optical coherence tomography. Science 1991;254:1178–81.

7. Choi BJ, Matsuo Y, Aoki T, et al. Coronary endothelial dysfunction is associated with inflammation and vasa vasorum proliferation in patients with early atherosclerosis. Arterioscler Thromb Vasc Biol 2014;34:2473–7.

8. Nishimiya K, Matsumoto Y, Takahashi J, et al. In vivo visualization of adventitial vasa vasorum of the human coronary artery on optical frequency domain imaging. Circ J 2014;78:2516–8.

9. Herrmann J, Lerman LO, Rodriguez-Porcel M, et al. Coronary vasa vasorum neovascularization precedes epicardial endothelial dysfunction in experimental hypercholesterolemia. Cardiovasc Res 2001;51:762–6.

10. Tearney GJ, Regar E, Akasaka T, et al., for the IWG-IVOCT. Consensus standards for acquisition, measurement, and reporting of intravascular optical coherence tomography studies: a report from the International Working Group for Intravascular Optical Coherence Tomography Standardization and Validation. J Am Coll Cardiol 2012;59:1058–72.

11. Tanaka A, Imanishi T, Kitabata H, et al. Morphology of exertion-triggered plaque rupture in patients with acute coronary syndrome: an optical coherence tomography study. Circulation 2008;118:2368–73.

12. Kitabata H, Tanaka A, Kubo T, et al. Relation of microchannel structure identified by optical coherence tomography to plaque vulnerability in patients with coronary artery disease. Am J Cardiol 2010;105:1673–8.

13. Tahara S, Morooka T, Wang Z, et al. Intravascular optical coherence tomography detection of atherosclerosis and inflammation in murine aorta. Arterioscler Thromb Vasc Biol 2012;32:1150–7.

14. Langheinrich AC, Michniewicz A, Sedding DG, et al. Correlation of vasa vasorum neovascularization and plaque progression in aortas of apolipoprotein E(-/-)/low-density lipoprotein(-/-) double knockout mice. Arterioscler Thromb Vasc Biol 2006;26:347–52.

15. Moulton KS, Vakili K, Zurakowski D, et al. Inhibition of plaque neovascularization reduces macrophage accumulation and progression of advanced atherosclerosis. Proc Natl Acad Sci U S A 2003;100:4736–41.

16. Williams JK, Armstrong ML, Heistad DD. Vasa vasorum in atherosclerotic coronary arteries: responses to vasoactive stimuli and regression of atherosclerosis. Circ Res 1988;62:515–23.

17. Kwon HM, Sangiorgi G, Ritman EL, et al. Adventitial vasa vasorum in balloon-injured coronary arteries: visualization and quantitation by a microscopic three-dimensional computed tomography technique. J Am Coll Cardiol 1998;32:2072–9.

18. Naghavi M, Libby P, Falk E, et al. From vulnerable plaque to vulnerable patient: a call for new definitions and risk assessment strategies: part I. Circulation 2003;108:1664–72.

19. Heistad DD, Marcus ML. Role of vasa vasorum in nourishment of the aortic wall. Blood Vessels 1979;16:225–38.

20. Gössl M, Beighley PE, Malyar NM, Ritman EL. Role of vasa vasorum in transendothelial solute transport in the coronary vessel wall: a study with cryostatic micro-CT. Am J Physiol Heart Circ Physiol 2004;287:H2346–51.

21. Uemura S, Ishigami K, Soeda T, et al. Thin-cap fibroatheroma and microchannel findings in optical coherence tomography correlate with subsequent progression of coronary atheromatous plaques. Eur Heart J 2012;33:78–85.

22. Virmani R, Kolodgie FD, Burke AP, et al. Atherosclerotic plaque progression and vulnerability to rupture: angiogenesis as a source of intraplaque hemorrhage. Arterioscler Thromb Vasc Biol 2005;25:2054–61.

23. Wilens SL, Malcolm JA, Vazquez JM. Experimental infarction (medial necrosis) of the dog's aorta. Am J Pathol 1965;47:695–711.

24. Wolinsky H, Glagov S. Nature of species differences in the medial distribution of aortic vasa vasorum in mammals. Circ Res 1967;20:409–21.

25. Gossl M, Lerman LO, Lerman A. Frontiers in nephrology: early atherosclerosis—a view beyond the lumen. J Am Soc Nephrol 2007;18:2836–42.

26. Kolodgie FD, Gold HK, Burke AP, et al. Intraplaque hemorrhage and progression of coronary atheroma. N Engl J Med 2003;349:2316–25.

27. Kwon HM, Sangiorgi G, Ritman EL, et al. Enhanced coronary vasa vasorum neovascularization in experimental hypercholesterolemia. J Clin Invest 1998;101:1551–6.

28. Drinane M, Mollmark J, Zagorchev L, et al. The antiangiogenic activity of rPAI-1(23) inhibits vasa vasorum and growth of atherosclerotic plaque. Circ Res 2009;104:337–45.

29. Ritman EL, Lerman A. The dynamic vasa vasorum. Cardiovasc Res 2007;75:649–58.

30. Kashiwagi M, Liu L, Chu KK, et al. Feasibility of the assessment of cholesterol crystals in human macrophages using micro optical coherence tomography. PLoS One 2014;9:e102669.

31. Tearney GJ. OCT imaging of macrophages: a bright spot in the study of inflammation in human atherosclerosis. J Am Coll Cardiol Img 2015;8:73–5.

KEY WORDS optical coherence tomography, plaque progression, plaque rupture, vasa vasorum, vulnerable plaque

APPENDIX For a supplemental figure, please see the online version of this article.